



1 A systematic examination of the relationships between CDOM and
2 DOC in inland waters in China

3 Kaishan Song¹, Ying Zhao^{1,2}, Zhidan Wen¹, Chong Fang^{1,2}, Yingxin Shang¹

4 ¹Northeast Institute of Geography and Agroecology, CAS, Changchun, 130102, China

5 ² University of Chinese Academy of Sciences, Beijing 100049, China

6 Corresponding author's E-mail: songks@iga.ac.cn; Tel: 86-431-85542364

7

8 **Abstract:** Chromophoric dissolved organic matter (CDOM) plays a vital role in the
9 biogeochemical cycle in aquatic ecosystems. The relationship between CDOM and
10 dissolved organic carbon (DOC) has been investigated, and the significant
11 relationship lays the foundation for the estimation of DOC using remotely sensed
12 imagery data. An algorithm has been developed to retrieve DOC via CDOM
13 absorption (a_{CDOM}) at 275 and 295 nm for coastal waters, but it is still unclear for the
14 relationship between DOC and a_{CDOM} in other types of waters. The current study
15 examined the samples from freshwater lakes, saline lakes, rivers and streams, urban
16 water bodies, and ice-covered lakes in China. The regression model slopes for DOC
17 versus $a_{CDOM}(275)$ ranged from extreme low 0.33 (highly saline lakes) to 1.03 (urban
18 waters) and 3.13 (river waters). The low values were observed in saline lake waters
19 and waters from semi-arid or arid regions where strong photo-bleaching is expected
20 due to thin ozone layers, less cloud cover, longer water residence time and daylight
21 hours. In contrast, high values were found in waters developed in wetlands or forest in
22 Northeast China, where massive organic matter was transported from catchment to



23 waters. The study also demonstrated that stronger relationships between CDOM and
24 DOC were revealed when $a_{\text{CDOM}(275)}$ were sorted by the ratio of $a_{\text{CDOM}(250)}$ to
25 $a_{\text{CDOM}(365)}$, which is a tracer for the CDOM absorption with respect to its
26 composition, and the determination of coefficient of the regression models ranged
27 from 0.78 to 0.99 for different groups of waters. Our results indicated the
28 relationships between CDOM and DOC are variable for different inland waters, and
29 therefore remote sensing models for DOC estimation through linking with CDOM
30 absorption need to be tailored according to water types.

31

32 **Keywords:** Absorption, CDOM, DOC, regression slope, saline water, fresh water

33



34 **1. Introduction**

35 Compared with other terrestrial ecosystems, e.g., forest and grassland, inland waters
36 only occupy a small fraction (3.5%) of the earth surface (Verpoorter et al., 2014).
37 However, they play a disproportional role for the global carbon cycling with respect
38 to carbon transportation, transformation and carbon storage (Tranvik et al., 2009;
39 Verpoorter et al., 2014; Yang et al., 2015). According to Tranvik et al. (2009), 2.9 Pg
40 C was transported from terrestrial ecosystems to inland waters every year, of which
41 about 0.6 Pg C was buried in the lake sediment, 1.4 Pg C was released into the air as
42 CO₂ or CH₄, and the rest of 0.9 Pg C was exported to the ocean via river channels.
43 However, the amount of dissolved organic carbon (DOC) stored in the inland waters
44 is still unclear or the uncertainty is still needed to be evaluated (Tranvik et al., 2009).
45 Determination DOC concentration is straightforward through field sampling and
46 laboratory analysis (Findlay and Sinsabaugh, 2003). However, there are millions of
47 lakes in the world, and many of them are remote and inaccessible, making it
48 impossible to evaluate DOC concentration using routine approach (Cardille et al.,
49 2013; Brezonik et al., 2015). Researchers have found that remote sensing might
50 provide a promising tool for quantification of DOC of inland waters at large scale
51 through linking DOC with chromophoric dissolved organic matter (CDOM),
52 particularly for these inland waters situating in remote region with less accessibility
53 (Cole et al., 2007; Tranvik et al., 2009; Kutser et al., 2015; Brezonik et al., 2015).

54 CDOM is one of the largest bioactive reservoirs of organic matter on the earth
55 (Para et al., 2010), influencing light transmittance in aquatic ecosystems (Vodacek et



56 al., 1997; Williamson and Rose, 2010). As one of the optically active constituents
57 (OACs) in waters, CDOM can be estimated through remotely sensed signals (Yu et al.,
58 2010; Kutser et al., 2015), and is acted as a proxy in many regions for the amount of
59 DOC in the water column. As shown in Fig.1, CDOM and DOC in the aquatic
60 ecosystems are mainly originated from external (allochthonous) and internal
61 (autochthonous) sources, in addition to directly discharge from anthropogenic
62 activities (Zhou et al., 2016). Generally, the autochthonous CDOM is essentially
63 originated from algae and macrophytes, and mainly consists of various compounds of
64 low molecular weights (Findlay and Sinsabaugh, 2003; Zhang et al., 2009). While, the
65 allochthonous CDOM is mainly derived from the surrounding terrestrial ecosystems,
66 and it comprises a continuum of small organic molecules to highly polymeric humic
67 substances with compounds typically ranging from 100 to 100,000 Da. In terms of
68 CDOM originates from anthropogenic, it contains fatty acid, amino acid and sugar,
69 thus the composition of CDOM is more complex than that from natural systems
70 (Zhou et al., 2016; Zhao et al., 2016). Hydrological factor also affects the DOC and
71 CDOM characteristic. The concentrations of and the relationship between CDOM and
72 DOC in river waters depend on many factors, in which the water type, the seasonality
73 and climatology, the typology of the water, the surrounding landscapes. Particularly,
74 the discharge and catchment area are the most important ones (Neff et al., 2006;
75 Spencer et al., 2012; Alvarez-Cobelas et al., 2012).

76 **[Insert Fig.1 about here]**

77 CDOM is a major light-absorbing substance, which is responsible for much of the



78 color in waters (Reche et al., 1999). The chemical structure and origin of CDOM can
79 be characterized by its absorption coefficients ($a_{CDOM}(\lambda)$) and spectral slopes (De
80 Haan and De Boer, 1987; Helms et al., 2008). Weishaar et al. (2003) has proven that
81 the carbon specific absorption coefficient at 254 nm, e.g., $SUVA_{254}$ is a good tracer
82 for the aromaticity of humic acid in CDOM, while the ratio of CDOM absorption at
83 250 to 365 nm ($a_{CDOM}(250/365)$, herein, M values) has been successfully used to track
84 the changes in DOM molecule weight (De Haan and De Boer, 1987; Zhang et al.,
85 2010) and absorption intensity (Song et al., 2013). Biodegradation and
86 photodegradation are the major processes to determine the transformation and
87 composition of CDOM (Findlay and Sinsabaugh, 2003). With prolonged sunlight
88 absorbed by CDOM, some of the colored fraction is lost by the photobleaching
89 processes (Miller et al., 1995; Zhang et al., 2010), which can be measured by the light
90 absorbance decreasing at some specific (diagnostic) wavelength, e.g., 250, 254, 275,
91 295, 365 or 440 nm. It should be noted that $a_{CDOM}(440)$ is usually used by remote
92 sensing community due to this wavelength is less affected by phytoplankton (Lee et
93 al., 2002). Under this circumstance, the relationship between CDOM and DOC varies
94 since CDOM loses color while the variation of DOC concentration is almost
95 negligible. Saline or brackish lakes in the arid or semi-arid regions generally expose
96 to longer sunlight radiation, thus CDOM absorbance decreases, while DOC is
97 accumulated due to the longer residence time (Curtis et al., 1997; Song et al., 2013;
98 Wen et al., 2016). Compared to photodegradation on CDOM, the biodegradation
99 processes by microbes are much complicated, and extracellular enzymes are the key



100 substance required to decompose the high-molecular-weight CDOM into
101 low-molecular-weight substrates (Findlay and Sinsabaugh, 2003; Romera-Castillo et
102 al., 2012). With compositional change, the absorption feature of CDOM and its
103 relation to DOC varies correspondingly, but the relationship between CDOM and
104 DOC is far from solved (Gonnelli et al., 2013). In addition, the $SUVA_{254}$ and
105 $a_{CDOM}(250/365)$ may be used to classify CDOM into different groups and enhance the
106 relationship with DOC based on CDOM absorption grouping.

107 Some studies have researched the spatial and seasonal variations of CDOM and
108 DOC in ice free season in lakes, rivers and oceans (Vodacek et al., 1997; Neff et al.,
109 2006; Stedmon et al., 2011; Brezonik et al., 2015), but less is known about saline
110 lakes (Song et al., 2013; Wen et al., 2016), particularly urban waters influenced by
111 sewage effluent and waters with ice cover in winter (Belzile et al., 2000, 2002; Zhao
112 et al., 2016). The relationship between DOC and CDOM lays the foundation for the
113 remote sensing estimation of DOC in both inland waters (Yu et al., 2010; Griffin et al.,
114 2011; Zhu et al., 2014; Brezonik et al., 2015) and marine (Hoge et al., 1996; Bricaud
115 et al., 2012; Nelson et al., 2012). The significant relationship between CDOM and
116 DOC was observed in the Gulf of Mexico, and stable regression model was
117 established between DOC and $a_{CDOM}(275)$ and $a_{CDOM}(295)$ (Fichot and Benner 2011).
118 Similar results were also found in other estuaries along a salinity gradient, for
119 example the Finish Gulf (Kowalczuk et al., 2006) and the Chesapeake Bay (Le et al.,
120 2013). However, Chen et al. (2004) found that the relationship between CDOM and
121 DOC was not conservative due to estuarine mixing or photo-degradation. Similar



122 arguments were raised for Congo River (Spencer et al. 2009) and waters across
123 mainland USA (Spencer et al., 2012). The study on the relationship between DOC and
124 CDOM in Lake Taihu found a relatively stable relationship for water samples
125 collected in different seasons except winter (Jiang et al. 2012). However, seasonal
126 variations were observed in some studies due to the mixing of various endmembers of
127 CDOM from different terrestrial ecosystems and internal source (Zhang et al., 2010;
128 Spencer et al., 2012; Zhou et al., 2016). Along with laboratory measurements,
129 portable instruments deployed in river or streams provide great potential to quantify
130 DOC and CDOM at very dynamic manner (Lee et al., 2015; Yu et al., 2016).

131 According to Fig.1, the proposed hypothesis suggests that the main source of
132 CDOM and DOC in different waters vary, coupled with biogeochemical processes
133 (photobleaching and microbial degradation), resulting in the compositional
134 differences, and ultimately affects CDOM absorption and its relationship with DOC.
135 Hydrological feature and anthropogenic processes further cause the relationship
136 between CDOM and DOC varies both in time and space. Remote sensing technology
137 has increasingly played a vital role in quantifying carbon cycling in inland waters
138 (Tranvik et al., 2009; Raymond et al., 2013). However, the prerequisite is to
139 systematically examine the relationship between CDOM and DOC. In this study, the
140 characteristics of DOC and CDOM in different inland waters across China were
141 examined to determine the spatial feature associated with landscape variations,
142 hydrologic conditions and saline gradients. The objectives of this study are to: 1)
143 examine the relationship between CDOM and DOC concentrations across a wide



144 range of waters with various physical, chemical and biological conditions, and 2)
145 develop a model for the relationship between DOC and CDOM based on the sorted
146 CDOM absorption feature, e.g., the ratio of $a_{\text{CDOM}}(250/365)$ with aiming to improve
147 the regression modeling accuracy.

148 **2. Materials and Methods**

149 The dataset is composed of five subsets of samples collected from various types of
150 waters across China (Table 1, Fig.2), which encompassed a wide range of DOC and
151 CDOM. The first dataset (n = 288; from early spring 2009 to late October 2014)
152 includes samples collected in freshwater lakes and reservoirs during the growing
153 season with various landscape types. The second dataset (n = 345; from early spring
154 2010 to late mid-September 2014) includes samples collected in brackish to saline
155 water bodies. The third dataset (n = 322; from early May 2012 to late October 2014)
156 includes samples collected in rivers and streams across different basins in China. In
157 addition, 69 samples were collected from three sections along the Songhua Rive, the
158 Yalu and the Hunjiang River during the ice free period in 2015 to examine the impact
159 of river flow on the relationship between DOC and CDOM (see Fig.S1 for location).
160 The fourth dataset (n = 328; from 2011 to 2014 in the ice frozen season) includes
161 samples collected in Northeast China in winter from both lake ice and underlying
162 waters. The fifth dataset (n = 221; from early May 2013 to mid-October 2014)
163 collects samples in urban water bodies, including lakes, ponds, rivers and streams,
164 which were severely polluted by sewage effluents. City maps and Landat imagery
165 data acquired in 2014 or 2015 were used to delineate urban boundaries with ArcGIS



166 10.0 (ESRI Inc., Redlands, California, USA), and water bodies in these investigated
167 cities constrained by urban boundaries were considered as urban water bodies. Except
168 river samples, the sampling dates, water body names and locations of other types of
169 water bodies were provided in supplementary Table S1-3.

170 **[Insert Fig.2 about here]**

171 **2.1 Water quality determination**

172 Water samples were collected approximately 0.5m below the water surface at each
173 station, generally locating in the middle of water bodies. Water samples were
174 collected in two 1 L amber HDPE bottles, and kept in coolers with ice packs in the
175 field and kept in refrigerator at 4°C after shipping back to the laboratory; all samples
176 were preprocessed (e.g., filtration, pH and electrical conductivity (EC) determination)
177 within two days in the laboratory. Water salinity was measured using DDS-307 EC
178 meter ($\mu\text{S}/\text{cm}$) at room temperature ($20\pm 2^\circ\text{C}$) and converted to *in situ* salinity units
179 (PSU) in the laboratory. Water samples were filtered using Whatman cellulose acetone
180 filter with pore size of 0.45 μm . Chlorophyll-a (Chl-a) was extracted and
181 concentration was measured using a Shimadzu UV-2050PC spectrophotometer (Song
182 et al., 2013). Total suspended matter (TSM) was determined gravimetrically using
183 pre-combusted Whatman GF/F filters with 0.7 μm pore size, details can be found in
184 Song et al. (2013). DOC concentrations were measured by high temperature
185 combustion (HTC) with water samples filtered through 0.45 μm Whatman cellulose
186 acetone filters (Song et al., 2013; Zhao et al., 2016a). The standards for dissolved total
187 carbon (DTC) were prepared from reagent grade potassium hydrogen phthalate in



188 ultra-pure water, while dissolved inorganic carbon (DIC) were determined using a
189 mixture of anhydrous sodium carbonate and sodium hydrogen carbonate. DOC was
190 calculated by subtracting DIC from DTC, both of which were measured using a Total
191 Organic Carbon Analyzer (TOC-VCPN, Shimadzu, Japan). Total nitrogen (TN) was
192 measured based on the absorption levels at 146 nm of water samples decomposed
193 with alkaline potassium peroxydisulfate. Total phosphorus (TP) was determined using
194 the molybdenum blue method after the samples were digested with potassium
195 peroxydisulfate (APHA, 1998). pH was measured using aPHS-3C pH meter at room
196 temperature ($20 \pm 2^\circ\text{C}$).

197 **2.2 CDOM absorption measurement**

198 All water samples were filtered at low pressure at two steps: 1) filtered at low
199 pressure through a pre-combusted Whatman GF/F filter ($0.7\mu\text{m}$), and 2) further
200 filtered through pre-rinsed 25 mm Millipore membrane cellulose filter ($0.22\ \mu\text{m}$).
201 Absorption spectra were obtained between 200 and 800 nm at 1 nm increment using a
202 Shimadzu UV-2600PC UV-Vis dual beam spectrophotometer (Shimadzu Inc., Japan)
203 through a 1 cm quartz cuvette (or 5 cm cuvette for ice melted water samples). Milli-Q
204 water was used as reference for CDOM absorption measurements. The Napierian
205 absorption coefficient (a_{CDOM}) was calculated from the measured optical density (OD)
206 of samples using Eq. (1):

$$207 \quad a_{\text{CDOM}}(\lambda) = 2.303[OD_{S(\lambda)} - OD_{(ml)}] / \beta \quad (1)$$

208 where β is the cuvette path length (0.01 or 0.05m) and 2.303 is the conversion factor
209 of base 10 to base e logarithms. To remove the scattering effect from the limited fine



210 particles remained in the filtered solutions, a necessitated correction was implemented
211 by assuming the average optical density over 740–750 nm to be zero (Babinet al.,
212 2003). All absorption measurements were conducted within 48 h after the samples
213 were shipped back to the laboratory. In addition, $SUVA_{254}$ and $a_{CDOM}(250/365)$ were
214 calculated to characterize and group CDOM with respect to their compositional
215 features and try to link DOC based on CDOM grouping.

216 **3. Results and discussion**

217 **3.1. Biological and geochemical characteristics**

218 The biological and geochemical properties in the water bodies are diverse. Chl-a
219 concentrations ($46.44 \pm 59.71 \mu\text{g/L}$) changed from 0.28 to $521.12 \mu\text{g/L}$, with the mean
220 of $46.44 \mu\text{g/L}$. TN and TP concentration were very high in fresh lake water, saline
221 lake water and particularly urban water bodies (Table 1), indicating that most of the
222 waters are heavily eutrophic. It is worth noting that Chl-a concentration was still high
223 $7.3 \pm 19.7 \mu\text{g/L}$ even in ice-covered lakes in winter from Northeast China, which
224 resulted from high TN ($4.3 \pm 5.4 \text{mg/L}$) and TP ($0.7 \pm 0.6 \text{mg/L}$) concentrations even
225 under ice cover. Electric conductivity (EC) and pH were high in the semi-arid and arid
226 regions, and they were 1067-41000 $\mu\text{s/cm}$ and 7.1-11.4, respectively. This is due to
227 specific regional hydro-geologic and climatic conditions. The results are consistent
228 with previous findings (Song et al., 2013; Wen et al., 2016). Overall, waters were
229 highly turbid with high TSM concentrations ($119.55 \pm 131.37 \text{mg/L}$), but there were
230 big variation between different types of waters (Table 1). Hydrographic conditions
231 exerted strong impact on water turbidity and TSM concentration, thus these two



232 parameters of river and stream samples were excluded in this study (Table 1). Large
233 variations of water quality parameters in the extensive geographic area, for example
234 in China, provide a more comprehensive dataset for examining the relationship
235 between DOC and CDOM, and the result is very helpful for establishing remote
236 sensing models to estimate DOC through CDOM absorption properties (Cardille et al.,
237 2013; Zhu et al., 2014; Kutser et al., 2015).

238 **[Insert Table 1 about here]**

239 **3.2. DOC concentrations in different types of waters**

240 DOC concentrations changed remarkably in the investigated waters (Table 1). DOC
241 concentrations were low in rivers, while they were much lower in ice melting waters
242 sampled in winter, which is consistent with previous findings (Bezilie et al., 2002;
243 Shao et al., 2016). It should be noted that large variations were observed in water
244 samples from rivers and streams (Table 2) (Raymond and Saiers, 2010; Ward et al.,
245 2012), due to the strong connection with hydrological condition and catchment
246 landscape features (Neff et al., 2006; Agren et al., 2007; Lee et al., 2015). Generally,
247 low DOC concentrations were found in rivers or streams in the drainage systems in
248 Tibetan Plateau or arid regions in Northwest China where soil contains relative low
249 level of soil organic carbon, but the high DOC concentrations were found in rivers or
250 streams surrounded by forest or wetlands in Northeast China. The similar findings
251 were reported by Agren et al. (2007, 2010). Among the five types of waters, relatively
252 higher DOC concentrations, ranging from 2.3 to 300.6 mg/L, were found in many
253 saline lakes, in the Songnen Plain, the HulunBuir Plateau and some areas in Tibetan



254 Plateau (see Fig.2 for location), which is consistent with previous investigations
255 conducted in the semi-arid or arid regions (Curtis et al., 1995; Song et al., 2013; Wen
256 et al., 2016). However, some of saline lakes supplied by snow melt water or ground
257 water exhibited relatively lower DOC concentrations even with high salinity.
258 Compared with samples collected in growing seasons, higher DOC concentrations
259 (7.3-720 mg/L) were observed in ice-covered water bodies, due to the condensed
260 effect caused by the DOC discharged from ice formation (Bezilie et al., 2002; Shao et
261 al., 2016). This condensed effect was particularly marked in these shallow water
262 bodies where ice forming remarkably condensed the DOC in the underlying waters
263 (Zhao et al., 2016a). Even in rivers or saline lakes, the concentrations of DOC
264 demonstrated obvious variations (Table 2). Comparatively, rivers from Qinghai
265 exhibited lower DOC concentration, while these from the Liaohe and Inner Mongolia
266 showed much higher DOC concentration (Table 2). Similarly, large DOC variations
267 were observed in saline lakes in different regions (Table 2). Much higher DOC
268 concentrations were found in saline lakes in Qinghai and Hulunbir, while relative low
269 concentrations were observed in Xilinguole Plateau and the Songnen Plain.

270 **[Insert Table 2 about here]**

271 **3.3. DOC versus CDOM for various types of waters**

272 *3.3.1 Freshwater lakes and reservoirs*

273 The relationship between DOC and CDOM has been researched based on CDOM
274 absorption spectra at different wavelengths (Fichot and Benner, 2011; Spencer et al.,
275 2012; Song et al., 2013; Brezonik et al., 2015). As suggested by Fichot and Benner



276 (2011), CDOM absorptions at 275 nm ($a_{CDOM275}$) and 295 nm ($a_{CDOM295}$) have
277 stable performances for DOC estimates for coastal waters. In current study, a strong
278 relationship ($R^2 = 0.85$) between DOC and $a_{CDOM(275)}$ was found in fresh lakes and
279 reservoirs (Fig.3a). However, the participation of $a_{CDOM(295)}$ explains very limited
280 variance, thus it is not considered in the regression models. Regression analyses of
281 water samples collected from different regions indicated that the slopes varied from
282 1.30 to 3.13 (Table 3). Water samples collected from East China and South China had
283 lower regression slope values (Table 3), and lakes and reservoirs were generally
284 mesotrophic or eutrophic (Huang et al., 2014; Yang et al. 2012, and references
285 therein). Phytoplankton degradation may contribute relative large portion of CDOM
286 and DOC in these water bodies (Zhang et al., 2010), due to the lower molecular
287 weight, its absorption is different from that derived from terrestrial systems (Helms et
288 al., 2008). Comparatively, fresh waters in Northeast and North China revealed larger
289 regression slopes (Table 3). Waters in Northeast China are surrounded by forest,
290 wetlands and grassland and therefore they generally exhibited high proportion of
291 colored fractions, CDOM (Helms et al., 2008). Soils in Northeast China are rich in
292 organic carbon, which may also contribute to high concentration of DOC and CDOM
293 in waters in this region (Jin et al., 2016; Zhao et al., 2016a). Compared with waters in
294 East and South China, waters in Northeast China showed less algal bloom due to low
295 temperature, thus autochthonous CDOM was less presented in waters in Northeast
296 China (Song et al., 2013; Zhao et al., 2016a). As suggested by Brezonik et al. (2015)
297 and Cardille et al. (2013), CDOM in the eutrophic waters or those with very short



298 resident time may show seasonal variation due to algal bloom or hydrological
299 variability, while CDOM in some oligotrophic lakes or those with long resident time
300 may show an opposite pattern.

301 **[Insert Table 3 about here]**

302 **[Insert Fig.3 about here]**

303 ***3.3.2 Saline lakes***

304 A strong relationship between DOC and $a_{CDOM}(275)$ ($R^2 = 0.85$) was demonstrated for
305 saline lakes (Fig.3b). However, compared to fresh waters, much lower regression
306 slope value (slope = 1.28) was found in saline lakes. Similar to fresh waters, the
307 slopes of most saline lakes exhibited large variations between different regions (Table
308 3), ranging from 0.86 in Tibetan waters to 2.83 in Songnen Plain waters (see Fig.2 for
309 location). As the extreme case, the slope value was only 0.33 as demonstrated in the
310 embedded diagram in Fig.3b. Saline lakes in semi-arid or arid regions generally
311 exhibit higher regression slope values, for example, west Songnen Plain (2.83),
312 Hulunbir Plateau and East Inner Mongolia Plateau (1.79). Whereas, waters in the west
313 Inner Mongolia Plateau (1.13), the Tibetan Plateau (0.86) exhibited low slope values
314 (Table 3), and the extreme low value was measured in the Lake Qinhai in Tibetan
315 Plateau. Lakes in Tarim Basin were affected by strong photo-bleaching, due to the
316 long resident time and strong solar radiation (Spencer et al., 2012; Song et al., 2013;
317 Wen et al., 2016). Thereby, smaller regression slopes were found and less colored
318 portion of DOC was presented in waters in semi-arid to arid regions, especially for
319 these closed lakes with enhanced photochemical processes (Spencer et al., 2012; Song



320 et al., 2013; Wen et al., 2016). The findings highlighted the difference in remote
321 sensing of DOC through CDOM absorption algorithm between saline and fresh lakes,
322 thereby different models should be established to accurately estimate DOC in waters
323 (Cardille et al., 2013; Brezonik et al., 2015).

324 *3.3.3 Streams and rivers*

325 Although some of the samples scattered from the regression line (Fig.3c), close
326 relationship between DOC and $a_{CDOM}(275)$ was found for samples collected in rivers
327 and streams. Compared with the other water types (Fig.3), rivers and streams
328 exhibited the highest regression slope value (slope = 3.13). Further regression analysis
329 with water samples sub-datasets collected in different regions indicated that slope
330 values presented large variability, ranging from 1.07 to 8.49. The lower regression
331 slope values were recorded in water samples collected in rivers and stream in
332 semi-arid and arid regions, such as the Tibetan Plateau, Mongolia Plateau and Tarim
333 Basin, while the higher values were found in samples collected in streams originated
334 from wetland and forest in Northeast China (Table 3). Rivers and streams in North,
335 East and South China generally exhibited intermediate values. In addition, water
336 samples in large river generally presented relatively low slope value; streams,
337 especially head water originating from forest and wetland dominated regions show
338 higher regression slope values (e.g., Branches from the Nenjiang and the Songhua
339 River in Table 3), which is consistent with the findings from Helm et al. (2008) and
340 Spencer et al. (2012). In fact, landscape pattern and soil organic carbon in the
341 catchment are important factors governing the terrestrial DOC and CDOM



342 characteristics in rivers and streams (Wilson and Xenopoulos, 2008; Jaffe et al., 2008;
343 Agren et al., 2010; Lai et al., 2016).

344 DOC concentration is strongly associated with hydrological conditions (Neff et al.
345 2006; Agren et al. 2007). Thereby, the relationships between CDOM and DOC in
346 river and stream waters are very variable (Lee et al., 2015) due to the hydrological
347 variability and catchment features (Agren et al., 2010; Spencer et al., 2009; 2012). To
348 investigate the dynamics of CDOM absorption and DOC concentrations, three
349 sections were investigated in three major rivers in Northeast China (see Figure S1 for
350 location). River flow exerted obvious effect on DOC and CDOM (Fig.4) and flood
351 impulse brought large amount of DOC and CDOM into river channels, which is
352 consistent with previous findings (Neff et al., 2006; Larson et al., 2007). As shown in
353 Fig.4, the relationship between river flows and DOC is rather complicated, which is
354 mainly caused by the land use, soil properties, relief, slope, the proportion of wetlands
355 and forest, climate and hydrology of the catchments (Neff et al., 2006; Sobek et al.,
356 2007; Spencer et al., 2012; Zhou et al., 2016), with additional influence by sewage
357 discharge into rivers. The relationships between DOC and $a_{CDOM}(275)$ in sections
358 along three rivers in Northeast China were demonstrated in Fig.5. The sampling point
359 in the Yalu River is near the river head source, thus strong relationship was exhibited
360 with large slope (Fig.5a), due to that the DOC and CDOM were fresh and less
361 disturbed by pollution from anthropogenic activities (Spencer et al., 2012; Shao et al.,
362 2016). The relationship between DOC and $a_{CDOM}(275)$ in the Songhua River at Harbin
363 City section was much scattered (Fig.5c) and this is mainly attributed to both point



364 and non-point source pollution that cause the composition and colored fractions of
365 DOC and DOM much varied comparing to river head waters with less human
366 disturbance. Similar mechanisms are further detailed in section 3.3.4 with urban
367 waters. With respect to Fig.5b, it is an in-between case. The sampling point was
368 affected by effluent from Baishan City, thus the coefficient of determination ($R^2=$
369 0.822) and the regression slope (3.72) were lower than that from the Yalu River at
370 Changbai point, while higher than that from the Songhua River at Harbin point.
371 Thereby, both spatial and temporal changes of the relationships between DOC and
372 CDOM were observed, and anthropogenic activities further complicated the
373 relationship.

374 **[Insert Fig.4 and Fig.5 about here]**

375 **3.3.4 Urban waters**

376 Relative close relationship between DOC and $a_{CDOM}(275)$ was revealed in urban
377 waters (Fig.3d, $R^2= 0.71$), where it was much scattered compared with other water
378 types (Fig.3), particularly for water samples with DOC concentration less than 60
379 mg/L. Similarly, regression slope values changed remarkably, ranging from 0.87 to
380 2.45. It is apparent that urban waters are severely impacted by human activities,
381 particularly sewage, effluents and runoff from urban impervious surface containing
382 large amount of DOM (Yang et al. 2008; Zhao et al., 2016b, and references therein).
383 High nutrients also usually result in algal bloom in most urban water bodies (Chl-a
384 range: 1.0-521.1 $\mu\text{g/L}$; average: 38.9 $\mu\text{g/L}$). Thereby, DOC and CDOM derived from
385 phytoplankton may also contribute a portion that should not be neglected (Xing et al.



386 2006; Zhang et al., 2010; Zhao et al., 2016b). More or less affected by sewage
387 effluent, the DOM in urban waters is much complex than those from natural water
388 bodies. Thus, a large variation of the relationship between DOC and $a_{\text{CDOM}(275)}$ was
389 found in urban waters.

390 *3.3.5 Ice covered lakes and reservoirs*

391 The closest relationship ($R^2 = 0.93$) between DOC and $a_{\text{CDOM}(275)}$ was recorded in
392 waters beneath ice covered lakes and reservoirs in Northeast China (Fig.3e). It was
393 argued that the close relationship indicated the concurrent processes taken place for
394 DOC accumulation and CDOM biogeochemical activities (Finlay et al., 2003;
395 Stedmon et al., 2011). The strong positive correlations between DOC and $a_{\text{CDOM}275}$ is
396 probably due to ice formation condensed these two parameters. The other possible
397 explanation was that ice and snow cover shielded out most of the solar radiation that
398 might cause a series of biochemical process for CDOM contained in water; further,
399 the inflows and direct rainfall over lakes or reservoirs also diminished, thus causing
400 limited effect on DOC and CDOM composition (Uusikiv et al., 2010; Belzile et al.,
401 2002). Further, the autochthonous DOC and CDOM in ice covered waters were also
402 limited due to the relatively weak primary production in winter ($\text{Chl-a} = 7.3 \mu\text{g/L}$),
403 resulting in much close relationship in winter waters.

404 Comparatively, a weak relationship between DOC and $a_{\text{CDOM}(275)}$ was
405 demonstrated in ice melting waters (Fig.3f), which was probably due to the ice/water
406 depth ratio causing variation of dissolved components expelled during ice formation.
407 The other reason is the biologically derived DOC in the ice matrix, which changes



408 with the variation of light and nutrient (Arrigo et al., 2010; Zhang et al., 2010).
409 Apparently, CDOM from ice melting waters were mainly originated from maternal
410 water during the ice formation, also from algal biological processes (Stedmon et al.,
411 2011; Arrigo et al., 2010). Similarly, snow cover, and nutrients in the ice also causes
412 the variation of biochemical processes that ultimately complicate the relationship
413 between DOC and CDOM (Bezilie et al., 2002; Spencer et al., 2009). Interestingly,
414 the regression slopes for ice samples (1.35) and under lying water sample (1.27) are
415 very close. In addition, there was a significant relationship between DOC in ice and
416 underlying waters ($R^2 = 0.86$), indicating the dominant components of CDOM and
417 DOC in the ice are from maternal underlying waters.

418 **3.3.6 DOC versus $a_{CDOM}(440)$**

419 CDOM absorption at 440 nm, i.e., $a_{CDOM}(440)$, is usually used as a surrogate to
420 represent its concentration (Bricaud et al., 1981; Babin et al., 2003), and widely used
421 in remote sensing community to quantify CDOM in waters (Lee et al., 2002; Binding
422 et al., 2008; Zhu et al., 2014). Significant relationships between DOC and $a_{CDOM}(440)$
423 were found in different types of waters (Fig.5). Compared to DOC versus $a_{CDOM}(275)$,
424 the relationships were more scattered due to the weak CDOM absorption at longer
425 wavelength (Bricaud et al., 1981; Binding et al., 2008). Through comparing Fig.3 with
426 Fig.6, it can be found that the overall relationships between DOC and CDOM at 440
427 nm resemble that at 275 nm for different types of waters. This has important
428 implication for remote sensing of DOC through the CDOM absorption as a bridge
429 (Zhu et al., 2014; Kuster et al., 2015; Brezonik et al., 2015). It is also worth noting



430 that most of the streams and rivers, including some of the urban water bodies, are not
431 suitable to quantify DOC through remote sensing imagery, and this is due to that
432 medium or even coarse resolution imagery cannot effectively capture the change of
433 signals from these small water bodies. However, the systematic examination for the
434 relationship between DOC and CDOM may help to quantify DOC through CDOM
435 absorption for deploying portable sensors in streams or rivers that can measure
436 CDOM absorption more accurately with dynamic manner (Spencer et al., 2012; Lee et
437 al., 2015; Ruhala and Zarnetske, 2016).

438 **[Insert Fig.6 about here]**

439 **3.4 CDOM molecular weight and aromaticity versus DOC**

440 **3.4.1 CDOM versus SUVA₂₅₄ and $a_{\text{CDOM}}(250/365)$**

441 The large variations of the slope of regression of DOC and $a_{\text{CDOM}}(275)$ in different
442 types of waters are probably due to the aromaticity and colored fractions in DOC
443 component (Spencer et al., 2009, 2012; Lee et al., 2015). SUVA₂₅₄ is an effective
444 indicator to characterize CDOM molecular weight. It may reflect the regression slope
445 value between DOC and CDOM absorption at 275 nm. It is obvious that SUVA₂₅₄ had
446 high values in fresh lakes, and waters from rivers or streams as well (Fig.7a). Saline
447 water and ice covered waters in Northeast China showed intermediate SUVA₂₅₄
448 values, while urban water and ice melting water exhibited lower values. The M value,
449 i.e., $a_{\text{CDOM}}(250/365)$ is another indicator to demonstrate the variation of molecular
450 weight and aromaticity of CDOM components (De Haan, 1993). Fresh lake water, river



451 and stream water, and urban water exhibited low M values (Fig.7b), which indicated
452 that larger aromaticity dominant for these three types of waters. Saline water, ice
453 covered water in Northeast China and ice melting water showed higher M values.
454 Since $SUVA_{254}$ is a proxy based on the ratio to DOC, it is inappropriate to establish
455 the relationship between CDOM and DOC based on the $SUVA_{254}$ classification.
456 Thereby, only M values, which reveal molecular weight and aromaticity, might help to
457 estimate DOC through CDOM absorption based on M threshold values for various
458 types of waters.

459 **[Insert Fig.7 about here]**

460 **3.4.2 Regression based on M values**

461 Regression models between DOC and $a_{CDOM}(275)$ were established based on M
462 threshold values, which were determined through trial test with respect to the
463 concentrations of DOC versus $a_{CDOM}(275)$. A relative weaker relationship between
464 DOC and $a_{CDOM}(275)$ was revealed in dataset where M values were less than 5
465 (Fig.8a). It should be noted that the high regression slope values appeared indifferent
466 groups of subset data (Fig.8a-h). The large range of M value ($0 < M < 4.0$) may explain
467 the scattered data pairs in Fig.8a and this is also the reason for the group with M
468 values ranging from 4 to 6 (Fig.8b). Better regression models appeared in groups with
469 intermediate M values (Fig.8c-f), with small range of regression slope values (1.15 -
470 1.38) and high determination of coefficients ($R^2 > 0.88$). Regression slope values
471 decreased with the increasing of M values (Fig.8g-h). Weak relationship between
472 DOC and $a_{CDOM}275$ appeared with relative lower or higher M values (Fig.8g). Very



473 significant relationship ($R^2 = 0.99$) was found with extremely high M values (Fig.8h).
474 Most of samples collected from these groups were presented in the embedded diagram
475 in Fig.3b, and the limited water bodies in the group may explain this coincidentally high
476 R^2 value. With more samples collected from different water bodies in this extreme
477 group, a weak relationship between DOC and $a_{CDOM}(275)$ may appear, while future
478 explorations are needed.

479 As noted in Fig.8c-f, close regression slopes implicate that a comprehensive
480 regression model with intermediate M value groups may be achieved. As expected, a
481 promising regression model (the diagram was not shown) between DOC and
482 $a_{CDOM275}$ was achieved ($y = 1.269x + 6.55$, $R^2 = 0.925$, $N = 998$, $p < 0.001$) with
483 pooled dataset shown in Figs.8c to 8f. Inspired by this idea, the relationship between
484 CDOM and DOC also examined with pooled data. As shown in Fig.9a, a significant
485 relationship between DOC and $a_{CDOM}(275)$ was obtained with the pooled dataset ($N =$
486 1504) collected from different types of inland waters. However, it should be noted
487 that the extremely high DOC samples may advantageously contribute the better
488 performance of the regression model. Thus, regression model excluding these eight
489 samples ($DOC > 300$ mg/L) was still significant (Fig.9b, $R^2 = 0.66$, $p < 0.01$). In
490 addition, regression model based on logarithm transformed data was established
491 (Fig.9c, $R^2 = 0.82$, $p < 0.01$). Most of the paired data sitting close to the regression
492 line except some scattered ones. This also implies that relative accurate regression
493 model for CDOM versus DOC can be achieved with data collected in inland waters at
494 global scale (Sobek et al., 2007), which might be helpful in quantifying DOC through



495 linking with CDOM absorption spectra, and the latter parameter can be estimated
496 from remote sensing data (Zhu et al., 2011; Kuster et al., 2015).

497 **[Insert Fig.8 and Fig.9 about here]**

498 **4. Conclusions**

499 As a powerful technology, remote sensing plays a crucial role in assessing CDOM and
500 DOC in water environment. In order to get accurate estimates of CDOM and DOC in
501 waters, it is necessary to get insight into the regional water optical properties for
502 developing semi-analytical or analytical models with remotely sensed data. Based on
503 the measurement of CDOM absorption spectral and DOC laboratory analysis, we
504 have systematically examined the relationships between CDOM and DOC in various
505 types of waters in China. This investigation showed that CDOM absorption varied
506 significantly. River waters and fresh lake waters exhibited high CDOM absorption
507 values and specific CDOM absorption ($SUVA_{254}$). On the contrast, saline lakes
508 illustrated low $SUVA_{254}$ values due to the long residence time and strong
509 photo-bleaching effects on waters in the semi-arid regions. Influenced by effluents
510 and sewage waters, CDOM from urban water bodies showed much complex
511 absorption feature. $SUVA_{254}$ for CDOM was lowest in ice melting water samples.

512 The current investigation indicated that the relationships between CDOM
513 absorption and DOC varied remarkably by showing very varied slope values of
514 regression models in various types of waters. The slope values of saline lakes and
515 urban waters were close to unity, slope values of river water were highest (~ 3.1), and
516 slope values of other water types were in between. It should also be highlighted that



517 head river water generally exhibit larger regression slope values, while rivers affected
518 by anthropogenic activities show lower slope values. When all the data set were
519 pooled together, the slope for regression model was about 1.3, but with much bigger
520 uncertainty ($R^2 = 0.66$). The accuracy of regression model between $a_{CDOM}(275)$ and
521 DOC was improved when CDOM absorptions were divided into different sub-groups
522 according to M values. Our finding highlights that remote sensing models for DOC
523 estimation based on the relationship between CDOM and DOC should consider water
524 types or cluster waters into several groups according to their absorption features.
525 More researches are still needed to further improved model accuracy.

526

527 **Acknowledgements**

528 The authors would like to thank financial supports from the National Basic Research
529 Program of China (No. 2013CB430401), Natural Science Foundation of China
530 (No.41471290), and “One Hundred Talents” Program from Chinese Academy of
531 Sciences granted to Dr. Kaishan Song. Thanks are also extended to all the staff and
532 students for their efforts in field data collection and laboratory analysis, and Dr. Hong
533 Yang to review and polish the English language. Last but not the least, the authors
534 would like to thank the editor and two anonymous referees for their valuable
535 comments that really help a lot in improving the manuscript.

536

537 **References**

538 Agren, A., Buffam, I., Jansson, M., Laudon, H., 2007. Importance of seasonality and



- 539 small streams for the landscape regulation of dissolved organic carbon export.
540 Journal of Geophysical Research, 112: G03003.
- 541 Agren, A., Haei, M., Kohler, S.J., Kohler, S.J., Bishop, K., Laudon, H., 2011.
542 Regulation of streamwater dissolved organic carbon (DOC) concentrations
543 during snowmelt; the role of discharge, winter climate and memory effects.
544 Biogeosciences, 7, 2901-2913.
- 545 Arrigo, K.R., Mock, T., Lizotte, M.P., 2010. Primary producers and sea ice, In *Sea Ice*,
546 edited by D.N. Thomas, and G.S. Dieckmann, pp. 283-326, second ed.,
547 Wiley-Blackwell, Oxford, UK.
- 548 Babin, M., Stramski, D., Ferrari, G. M., Claustre, H., Bricaud, A., Obolensky, G.,
549 Hoepffner, N., 2003. Variations in the light absorption coefficients of
550 phytoplankton, nonalgal particles, and dissolved organic matter in coastal waters
551 around Europe. Journal of Geophysical Research, 108(C7), 3211.
- 552 Belzile, C., Gibson, J.A.E., Vincent, W.F., 2002. Colored dissolved organic matter and
553 dissolved organic carbon exclusion from lake ice: implications for irradiance
554 transmission and carbon cycling. Limnology and Oceanography, 47(5),
555 1283–1293.
- 556 Binding, C.E., Jerome, J.H., Bukata, R.P., Booty, W.G., 2008. Spectral absorption
557 properties of dissolved and particulate matter in Lake Erie. Remote Sensing of
558 Environment, 112(4), 1702-1711.
- 559 Brezonik, P.L., Olmanson, L.G., Finlay, J.C., Bauer, M.E., 2015. Factors affecting the
560 measurement of CDOM by remote sensing of optically complex inland waters.



- 561 Remote Sensing of Environment, 157, 199-215.
- 562 Bricaud, A., Morel, A., Prieur, L., 1981. Absorption by dissolved organic matter of the
563 sea (yellow substance) in the UV and visible domains, *Limnology and*
564 *Oceanography*, 26(1), 43– 53.
- 565 Bricaud, A., Ciotti, A.M., Gentili, B., 2012. Spatial-temporal variations in
566 phytoplankton size and colored detrital matter absorption at global and regional
567 scales, as derived from twelve years of SeaWiFS data (1998–2009). *Global*
568 *Biogeochemical Cycles*, 26, GB1010, doi:10.1029/2010GB003952.
- 569 Cardille, J.A., Leguet, J.B., del Giorgio, P., 2013. Remote sensing of lake CDOM
570 using noncontemporaneous field data. *Canadian Journal of Remote Sensing*, 39,
571 118–126.
- 572 De Haan, H., 1993. Solar UV-light penetration and photodegradation of humic
573 substances in peaty lake water. *Limnology and Oceanography*, 1993, 38,
574 1072–1076.
- 575 De Haan, H., De Boer, T., 1987. Applicability of light absorbance and fluorescence as
576 measures of concentration and molecular size of dissolved organic carbon in
577 humic Laken Tjeukemeer. *Water Research*, 21, 731–734.
- 578 Duarte, C.M., Prairie, Y.T., Montes, C., Cole, J., Striegl, R., Melack, J., Downing, J.A.,
579 2008. CO₂ emission from saline lakes: A global estimates of a surprisingly large
580 flux. *Journal of Geophysical Research*, 113, G04041.
- 581 Fellman, J.B., Petrone, K.C., Grierson, F., 2011. Source, biogeochemical cycling, and
582 fluorescence characteristics of dissolved organic matter in an agro-urban estuary.



- 583 Limnology and Oceanography, 56(1), 243–256.
- 584 Ferrari, G.M., Tassan, S., 1992. Evaluation of the influence of yellow substance
585 absorption on the remote sensing of water quality in the Gulf of Naples: a case
586 study. International Journal of Remote Sensing, 13, 2177–2189.
- 587 Ferrari, G. M., Dowell. M. D., 1998. CDOM absorption characteristics with relation
588 to fluorescence and salinity in coastal areas of the Southern Baltic Sea. Estuarine,
589 Coastal and Shelf Science, 47, 91–105.
- 590 Fichot, C.G., Benner, R., 2011. A novel method to estimate DOC concentrations from
591 CDOM absorption coefficients in coastal waters. Geophysical Research Letter,
592 38, L03610.
- 593 Findlay, S.E.G., Sinsbaugh, R.L., 2003. Aquatic Ecosystems Interactivity of
594 Dissolved Organic Matter. Academic Press, San Diego, CA, USA.
- 595 Griffin, C.G., Frey, K.E., Rogan, J., Holmes, R.M., 2011. Spatial and interannual
596 variability of dissolved organic matter in the Kolyma River, East Siberia,
597 observed using satellite imagery. Journal of Geophysical Research, 116,
598 G03018.
- 599 Helms, J.R., Stubbins, A., Ritchie, J.D., Minor, E.C., Kieber, D.J., Mopper, K., 2008.
600 Absorption spectral slopes and slope ratios as indicators of molecular weight,
601 source, and photobleaching of chromophoric dissolved organic matter.
602 Limnology and Oceanography, 53, 955–969.
- 603 Jaffé R., McKnight, D., Maie, N., Cory, R., McDowell, W.H., Campbell, J.L., 2008.
604 Spatial and temporal variations in DOM composition in ecosystems: The



- 605 importance of long-term monitoring of optical properties. Journal of
606 Geophysical Research, 113, G04032.
- 607 Jin, X.L., Du, J., Liu, H.J., Wang, Z.M., Song, K.S., 2016. Remote estimation of soil
608 organic matter content in the Sanjiang Plain, Northeast China: The optimal band
609 algorithm versus the GRA-ANN model. Agricultural and Forest Meteorology,
610 218, 250–260.
- 611 Hoge, F.E., Lyon, P.E., 1996. Satellite retrieval of inherent optical properties by linear
612 matrix inversion of oceanic radiance models: An analysis of model and radiance
613 measurement errors. Journal of Geophysical Research-Oceans, 101(C7):
614 16631–16648.
- 615 Huang, C.C., Li, Y.M., Yang, H., Li, J.S., Chen, X., Sun, D.Y., Le, C.F., Zou, J., Xu,
616 L.J., 2014. Assessment of water constituents in highly turbid productive water by
617 optimization bio-optical retrieval model after optical classification. Journal of
618 Hydrology, 519, 1572-1583
- 619 Kowalczuk, P., Stedmon. C.A., Markager. S., 2006. Modeling absorption by CDOM
620 in the Baltic Sea from salinity and chlorophyll. Marine Chemistry, 101, 1–11.
- 621 Kowalczuk, P., Zablocka, M., Sagan, S., Kulinski, K., 2010. Fluorescence measured
622 in situ as a proxy of CDOM absorption and DOC concentration in the Baltic Sea.
623 Oceanologia, 52(3), 431–471.
- 624 Kutser, T., Verpoorter, C., Paavel, B., Tranvik, L.J., 2015. Estimating lake carbon
625 fractions from remote sensing data. Remote Sensing of Environment, 157,
626 138–146.



- 627 Lai, L., Huang, X., Yang, H., Chuai, X., Zhang, M., Zhong, T., Chen, Z., Chen, Y.,
628 Wang, X., Thompson, J.R., 2016. Carbon emissions from land-use change and
629 management in China between 1990 and 2010. *Science Advances*, 2(11),
630 e1601063.
- 631 Larson, J.H., Frost, P.C., Zheng, Z.Y., Johnston, C.A., Bridgham, S.D., Lodge, D.M.,
632 Lamberti, A.A., 2007. Effects of upstream lakes on dissolved organic matter in
633 streams. *Limnology and Oceanography*, 52(1), 60–69.
- 634 Le, C.F., Hu, C.M., Cannizzaro, J., Duan, H.T., 2013. Long-term distribution patterns
635 of remotely sensed water quality parameters in Chesapeake Bay. *Estuarine,
636 Coastal and Shelf Science*, 128(10), 93–103.
- 637 Lee, E.J., Yoo, G.Y., Jeong, Y., Kim, K.U., Park, J.H., Oh, N.H., 2015. Comparison of
638 UV–VIS and FDOM sensors for in situ monitoring of stream DOC
639 concentrations. *Biogeosciences*, 12, 3109–3118.
- 640 Lee, Z.P., Carder, K.L., Arnone, R.A., 2002. Deriving inherent optical properties from
641 water color: A multiband quasi-analytical algorithm for optically deep waters.
642 *Applied Optics*, 41(27), 5755–5777.
- 643 Jiang, G.J., Ma, R.H., Duan, H.T., 2012. Estimation of DOC Concentrations Using
644 CDOM Absorption Coefficients: A Case Study in Taihu Lake. *Environmental
645 Sciences*, 33(7), 2235–2243. (In Chinese with English abstract).
- 646 Markager, W., Vincent, W.F., 2000. Spectral light attenuation and absorption of UV
647 and blue light in natural waters. *Limnology and Oceanography*, 45(3), 642–650.
- 648 Mayorga, E., Aufdenkampe, A.K., Masiello, C.A., Krusche, A.V., Hedges, J.I., Quay,



- 649 P.D., Richey, J.E., Brown, T.A., 2005. Young organic matter as a source of
650 carbon dioxide outgassing from Amazonian rivers. *Nature*, 436(7050), 538-541.
- 651 Miller, W.L., Zepp, R.G., 1995. Photochemical production of dissolved inorganic
652 carbon from terrestrial organic matter: Significance to the oceanic organic
653 carbon cycle. *Geophysical Research Letter*, 22 (4), 417–420.
- 654 Neff, J.C., Finlay, J.C., Zimov, S.A., Davydov, S.P., Carrasco, J.J., Schuur, E.A.G.,
655 Davydova, A.I., 2006. Seasonal changes in the age and structure of dissolved
656 organic carbon in Siberian rivers and streams. *Geophysical Research Letter*, 33,
657 L23401.
- 658 Nelson, N.B., Siegel, D.A., Carlson, C.A., Swan, C.M., 2010. Tracing global
659 biogeochemical cycles and meridional overturning circulation using
660 chromophoric dissolved organic matter. *Geophysical Research Letter*, 37,
661 L03610, doi:10.1029/2009GL042325.
- 662 Para, J., Coble, P.G., Charriere, B., Tedetti, M., Fontana, C., Sempere, R., 2010.
663 Fluorescence and absorption properties of chromophoric dissolved organic
664 matter (CDOM) in coastal surface waters of the northwestern Mediterranean Sea,
665 influence of the Rhone River. *Biogeosciences*, 7, 4083–4103.
- 666 Raymond, P. A., Hartmann, J., Lauerwald, R., et al., 2013. Global carbon dioxide
667 emissions from inland waters. *Nature*, 503(7476), 355–359.
- 668 Raymond, P.A., Saiers, J.E., 2010. Event controlled DOC export from
669 forested watersheds. *Biogeochemistry*, 100(1-3), 197–209.
- 670 Reche, I., Pace, M., Cole, J.J., 1999. Relationship of trophic and chemical conditions



671 to photobleaching of dissolved organic matter in lake ecosystems.
672 Biogeochemistry, 44, 529-280.

673 Ruhala, S.S., Zarnetske, J.P., 2016. Using in-situ optical sensors to study dissolved
674 organic carbon dynamics of streams and watersheds: A review. Science of The
675 Total Environment, doi.org/10.1016/j.scitotenv.2016.09.113.

676 Stedmon, C.A., Thomas, D.N., Granskog, M.A., Kaartokallio, H., Papadimitriou, S.,
677 Kuosa, H., 2007. Characteristics of dissolved organic matter in Balticcoastal sea
678 ice: Allochthonous or autochthonous origins?, Environmental Science and
679 Technology, 41, 7273–7279.

680 Stedmon, C.A., Thomas, D.N., Papadimitriou, S., Granskog, M.A., Dieckmann, G.S.
681 2011. Using fluorescence to characterize dissolved organic matter in Antarctic
682 sea ice brines. Journal of Geophysical Research, 116, G03027.

683 Spencer, R.G.M., Stubbins, A., Hernes, P.J., Baker, A., Mopper, K., Aufdenkampe,
684 A.K., Dyda, R.Y., Mwamba, V.L., Mangangu, A.M., Wabakanghanzi, J.N., Six, J.,
685 2009. Photochemical degradation of dissolved organic matter and dissolved
686 ligninphenols from the Congo River. Journal of Geophysical Research, 114,
687 G03010.

688 Spencer, R.G.M., Butler, K.D., Aiken, G.R., 2012. Dissolved organic carbon and
689 chromophoric dissolved organic matter properties of rivers in the USA. Journal
690 of Geophysical Research, 117, G03001.

691 Song, K.S., Zang, S.Y., Zhao, Y., Li, L., Du, J., Zhang, N.N., Wang, X.D., Shao, T.T.,
692 Liu, L., Guan, Y., 2013. Spatiotemporal characterization of dissolved Carbon for



- 693 inland waters in semi-humid/semiarid region, China. *Hydrology and Earth*
694 *System Science*, 17, 4269–4281.
- 695 Shao, T.T., Song, K.S., Du, J., Zhao, Y., Ding, Z., Guan, Y., Liu, L., Zhang, B., 2016.
696 Seasonal variations of CDOM optical properties in rivers across the Liaohe Delta.
697 *Wetlands*, 36 (suppl.1): 181–192.
- 698 Tranvik, L.J., Downing, J.A., Cotner, J.B., et al., 2009. Lakes and reservoirs as
699 regulators of carbon cycling and climate. *Limnology and Oceanography*, 54(6),
700 2298–2314.
- 701 Uusikivi, J., Vahatalo, A.V., Granskog, M.A., Sommaruga, R., 2010. Contribution of
702 mycosporine-like amino acids and colored dissolved and particulate matter to
703 sea ice optical properties and ultraviolet attenuation. *Limnology and*
704 *Oceanography*, 55(2), 703–713.
- 705 Verpoorter, C., Kutser, T., Seekell, D.A., Tranvik, L.J., 2014. A global inventory of
706 lakes based on high-resolution satellite imagery. *Geophysical Research Letter*,
707 41, 6396–6402.
- 708 Vodacek, A., Blough, N.V., Degrandpre, M.D., Peltzer, E.T., Nelson, R.K., 1997.
709 Seasonal variation of CDOM and DOC in the Middle Atlantic Bight: terrestrial
710 inputs and photooxidation. *Limnology and Oceanography*, 42, 674–686.
- 711 Weishaar, J.L., Aiken, G.R., Bergamaschi, B.A., Fram, M.S., Fugii, R., Mopper, K.,
712 2003. Evaluation of specific ultraviolet absorbance as an indicator of the
713 chemical composition and reactivity of dissolved organic carbon.
714 *Environmental Science and Technology*, 37, 4702–4708.



- 715 Wen, Z.D., Song, K.S., Zhao, Y., Du, J., Ma, J.H., 2016. Influence of environmental
716 factors on spectral characteristic of chromophoric dissolved organic
717 matter(CDOM) in Inner Mongolia Plateau, China. *Hydrology and Earth System*
718 *Sciences*, 20, 787–801.
- 719 Williamson, C.E., Rose, K.C., 2010. When UV meets fresh water. *Science*, 329,
720 637–639.
- 721 Wilson, H., Xenopoulos, M.A., 2008. Ecosystem and seasonal control of stream
722 dissolved organic carbon along a gradient of land use. *Ecosystems* 11, 555–568.
- 723 Ward, N.D., Richey, J.E., Keil, R.G., 2012. Temporal variation in river nutrient and
724 dissolved lignin phenol concentrations and the impact of storm events on
725 nutrient loading to Hood Canal, Washington, USA. *Biogeochemistry*, 111(1-3),
726 629–645.
- 727 Ward, N.D., Keil, R.G., Medeiros, P.M., Brito, D.C., Cunha, A.C., Dittmar, T., Yager,
728 P.L., Krusche, A.V. and Richey, J.E., 2013. Degradation of terrestrially derived
729 macromolecules in the Amazon River. *Nature Geoscience*, 6(7), 530–533.
- 730 Xing, Y. P., Xie, P., Yang, H., Wu, A. P., Ni, L. Y., 2006. The change of gaseous
731 carbon fluxes following the switch of dominant producers from macrophytes to
732 algae in a shallow subtropical lake of China. *Atmospheric Environment*, 40,
733 (40), 8034–8043.
- 734 Yang, H., Andersen, T., Dörsch, P., Tominaga, K., Thrane, J.-E., Hessen, D. O., 2015.
735 Greenhouse gas metabolism in Nordic boreal lakes. *Biogeochemistry*, 126,
736 211–225.



- 737 Yang, H., Xie, P., Ni, L., Flower, R. J., 2011. Under estimation of CH₄ emission from
738 freshwater lakes in China. *Environmental Science & Technology*, 45, (10),
739 4203–4204.
- 740 Yang, H., Xing, Y., Xie, P., Ni, L., Rong, K., 2008. Carbon source/sink function of a
741 subtropical, eutrophic lake determined from an overall mass balance and a gas
742 exchange and carbon burial balance. *Environmental Pollution*, 151, (3),
743 559–568.
- 744 Yang, H., Xie, P., Ni, L., Flower, R. J., 2012. Pollution in the Yangtze. *Science*, 337,
745 (6093), 410–410.
- 746 Yu, Q., Tian, Y. Q., Chen, R.F., Liu, A., Gardner, G.B., Zhu, W.N., 2010. Functional
747 linear analysis of in situ hyperspectral data for assessing CDOM in
748 rivers. *Photogrammetric Engineering & Remote Sensing*, 76(10), 1147–1158.
- 749 Yu, X.L., Shen, F., Liu, Y.Y., 2016. Light absorption properties of CDOM in the
750 Changjiang (Yangtze) estuarine and coastal waters: An alternative approach for
751 DOC estimation. *Estuarine, Coastal and Shelf Science*, 181, 302–311.
- 752 Zhang, Y.L., Qin, B.Q., Zhu, G.W., Zhang, L., Yang, L.Y., 2007. Chromophoric
753 dissolved organic matter (CDOM) absorption characteristics in relation to
754 fluorescence in Lake Taihu, China, a large shallow subtropical lake.
755 *Hydrobiologia*, 581, 43–52.
- 756 Zhang, Y.L., Zhang, E.L., Yin, Y., Van Dijk, M.A., Feng, L.Q., Shi, Z.Q., Liu, M.L.,
757 Qin, B.Q., 2010. Characteristics and sources of chromophoric dissolved organic
758 matter in lakes of the Yungui Plateau, China, differing in trophic state and



759 altitude. *Limnology and Oceanography*, 55(6), 2645–2659.

760 Zhao, Y., Song, K.S., Wen, Z.D., Li, L., Zang, S.Y., Shao, T.T., Li, S.J., Du, J., 2016a.

761 Seasonal characterization of CDOM for lakes in semiarid regions of Northeast

762 China using excitation–emission matrix fluorescence and parallel factor analysis

763 (EEM - PARAFAC). *Biogeosciences*, 13, 1635–1645.

764 Zhao, Y., Song, K.S., Li, S.J., Ma, J.H., Wen, Z.D., 2016b. Characterization of CDOM

765 from urban waters in Northern-Northeastern China using excitation-emission

766 matrix fluorescence and parallel factor analysis. *Environmental Science and*

767 *Pollution Research*, 23, 15381–15394.

768 Zhu, W., Yu, Q., Tian, Y. Q., Chen, R.F., Gardner, G.B., 2011. Estimation of

769 chromophoric dissolved organic matter in the Mississippi and Atchafalaya river

770 plume regions using above-surface hyperspectral remote sensing. *Journal of*

771 *Geophysical Research: Oceans* (1978–2012), 116(C2), C02011.

772 Zhu, W.N., Yu, Q., Tian, Y. Q., et al., 2014. An assessment of remote sensing

773 algorithms for colored dissolved organic matter in complex freshwater

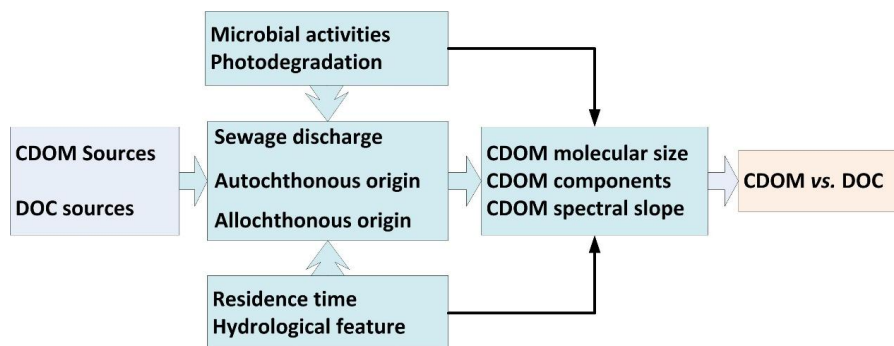
774 environments. *Remote Sensing of Environment*, 140, 766–778.

775



776 **Figures**

777 Fig.1. the diagram shows the regulating factors that influence the relationship between
778 CDOM and DOC.



779

780

781

782

783

784

785

786

787

788

789

790

791

792

793

794

795

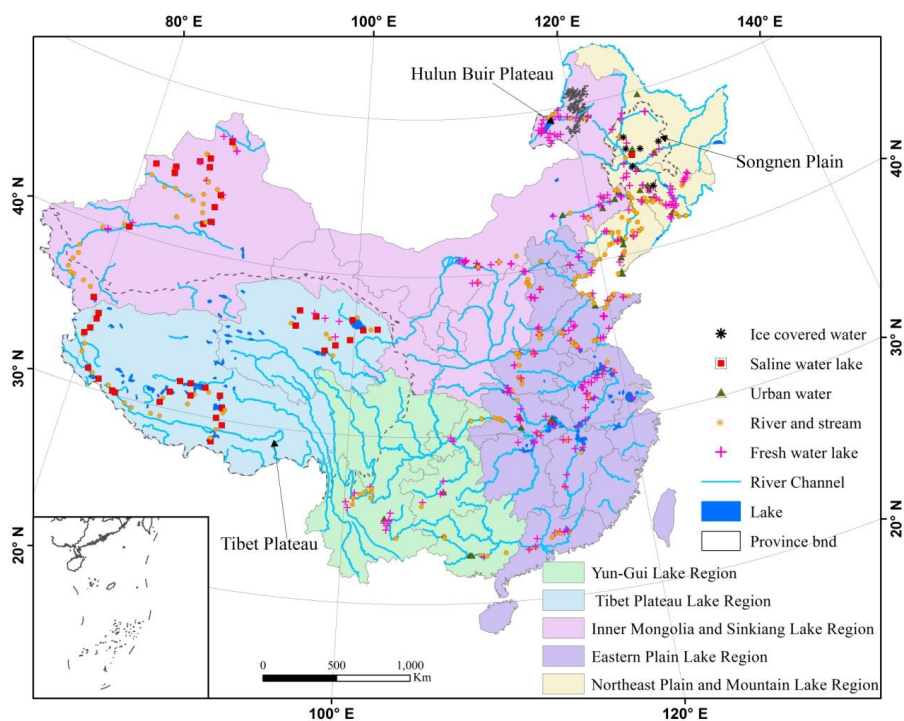
796

797

798



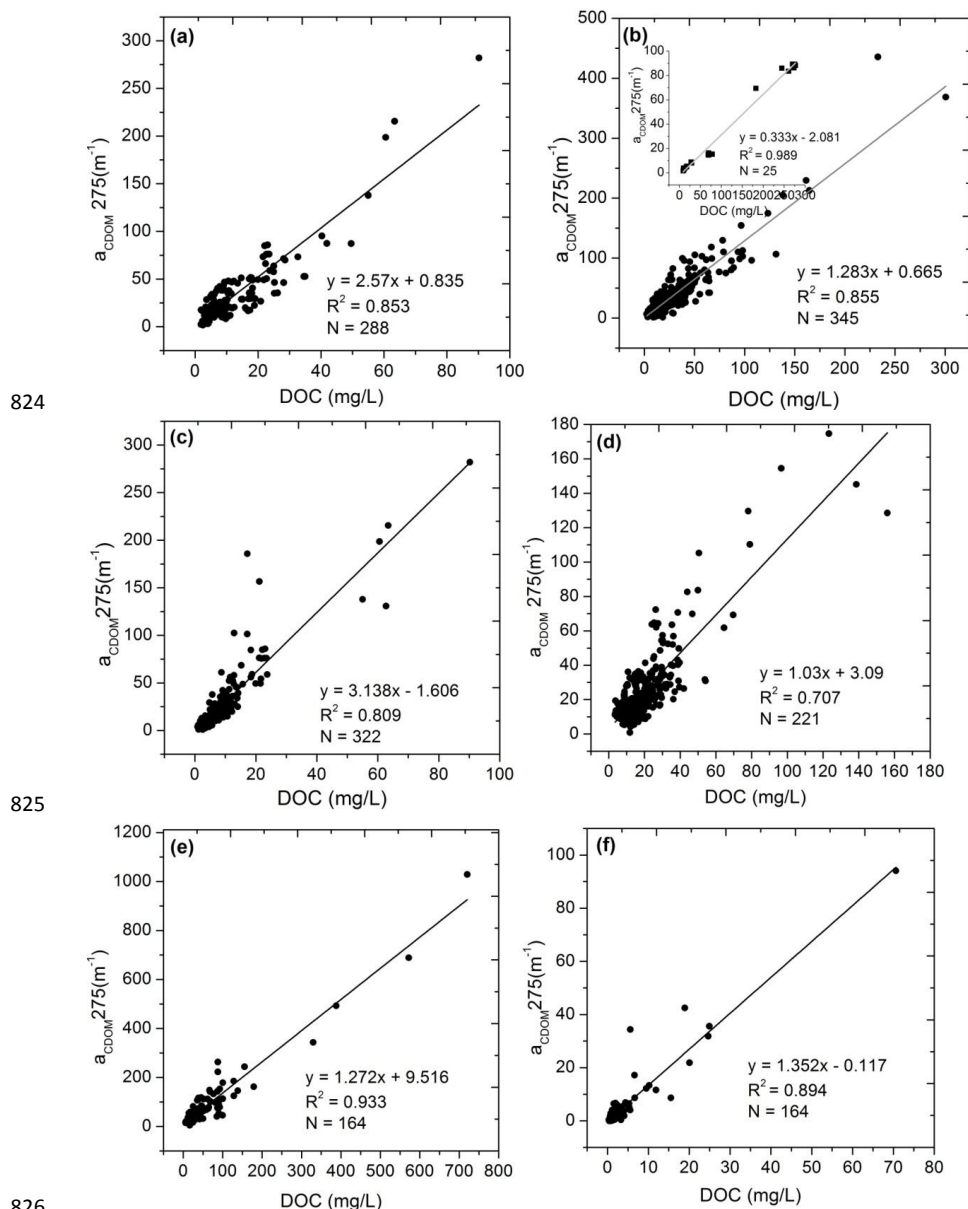
799 Fig.2. Water types and sample distributions across the mainland China. The dash line
800 shows the boundary of some typical geographic units.
801



802
803
804
805
806
807
808
809
810
811
812
813
814
815
816
817
818
819
820

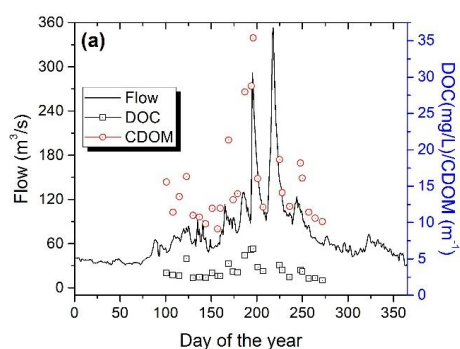


821 Fig.3. Relationship between DOC and $a_{\text{CDOM}}(275)$ in different types of inland waters,
 822 (a) fresh water lakes, (b) saline water lakes, (c) river and stream waters, (d) urban
 823 waters, (e) ice covered lake underlying waters, and (f) ice melting lake waters.

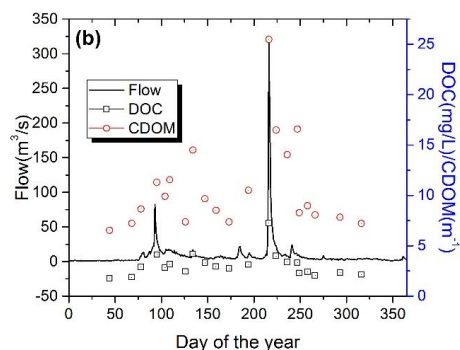




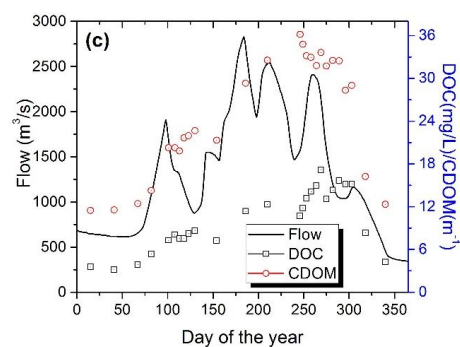
830 Fig.4. Flow dynamics for three rivers in Northeast China and corresponding DOC and
831 CDOM variations; (a) the Yalu River near Changbai County, (b) the Hunjiang River
832 with DOC and CDOM sampled at Baishan City, while the river flow gauge station is
833 near the Tonghua City, (c) the Songhua River at Harbin City. Note, the flow data for
834 the Yalu River and the Hunjiang River were the average values measured during
835 1970s, while the Songhua River was measured during 2000-2010.



836



837



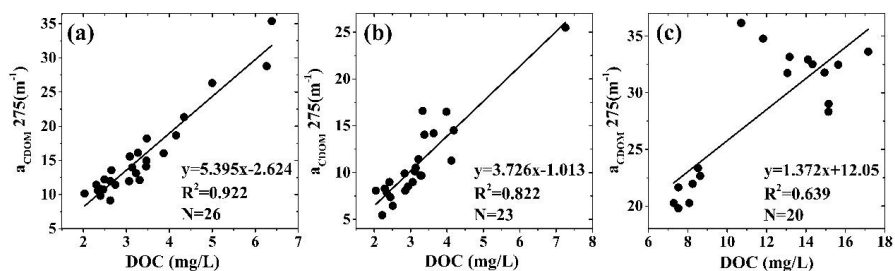
838

839

840



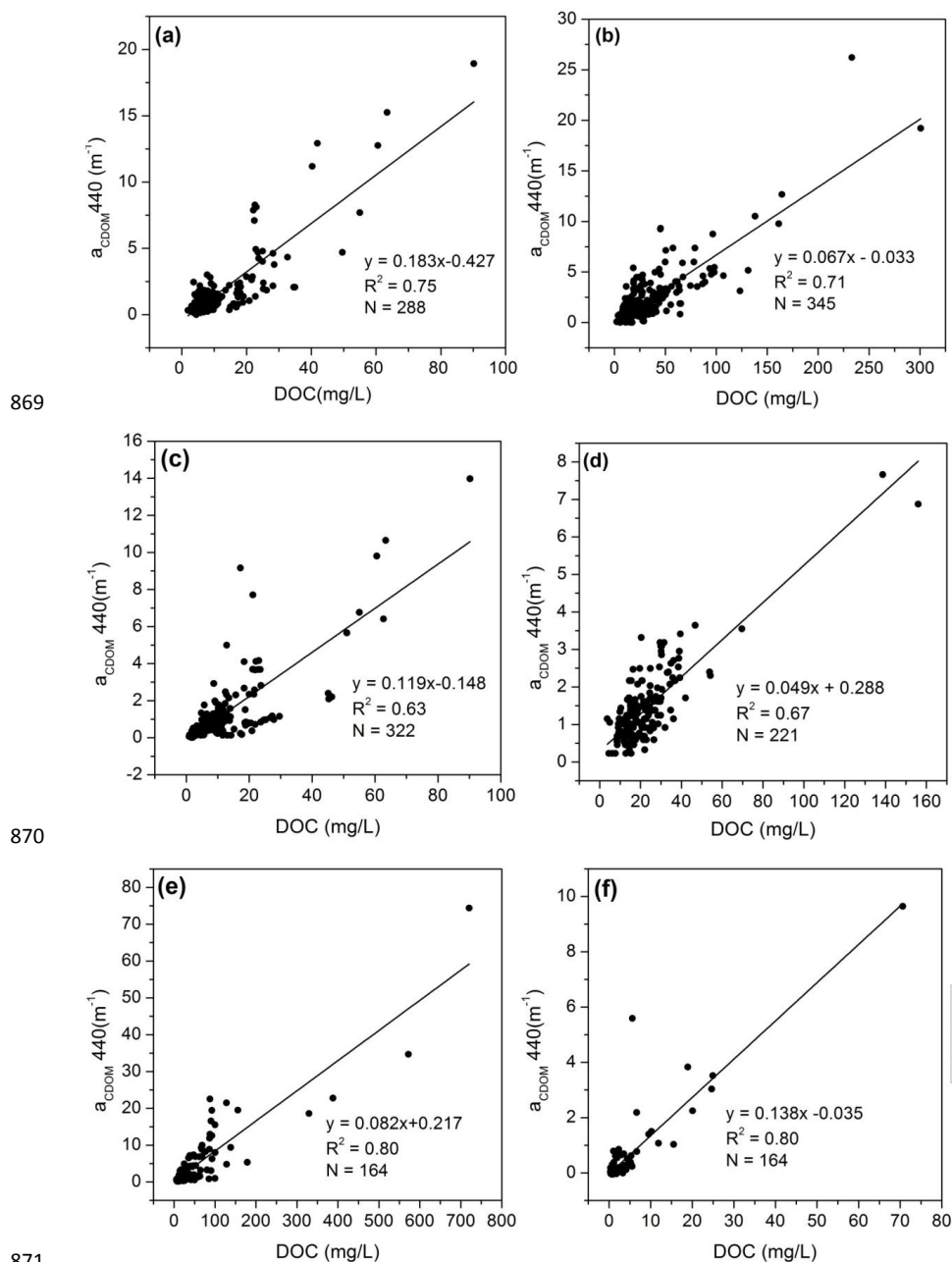
841 Fig.5. The relationships between $a_{CDOM,275}$ and DOC at sections across (a) the Yalu
842 River, (b) the Hunjiang River, and (c) the Songhua River. The samples were collected
843 at each station at about one week or around ten days in ice free season in 2015.



844
845
846
847
848
849
850
851
852
853
854
855
856
857
858
859
860
861
862
863
864
865

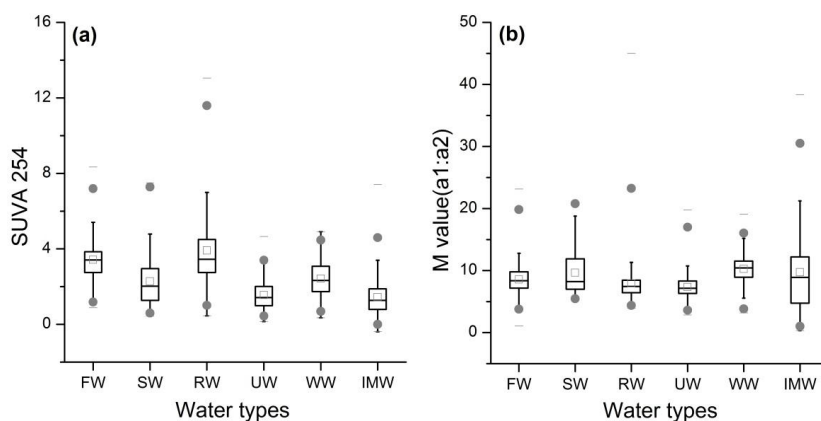


866 Fig.6. Relationship between DOC and $a_{\text{CDOM}}(440)$ in different types of inland waters,
867 (a) fresh water lakes, (b) saline water lakes, (c) river and stream waters, (d) urban
868 waters, (e) ice covered lake underlying waters, and (f) ice melting waters.





873 Fig.7. Comparison of (a) SUVA₂₅₄, and (b) M ($a_{250}:a_{365}$) values in various types of
874 inland waters. FW, fresh lake water; SW, saline lake water, RW, river or stream water;
875 UW, urban water; WW, ice covered winter water from Northeast China; IMW, ice
876 melt water from Northeast China.

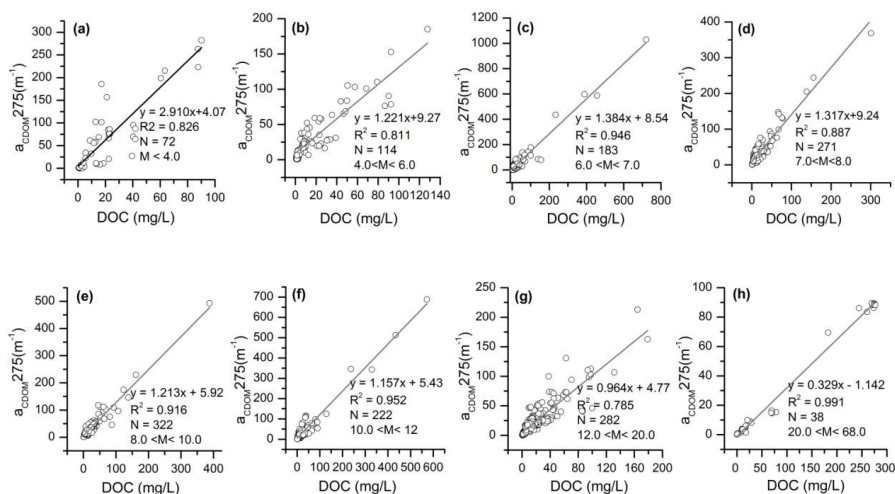


877
878
879
880
881
882
883
884
885
886
887
888
889
890
891
892
893
894
895
896
897
898
899
900
901
902



903 Fig.8. Relationship between DOC and $a_{CDOM,275}$ sorted by M ($a_{CDOM,250/365}$) values
 904 ranges, (a) $M < 4.0$, (b) $4.0 < M < 6.0$, (c) $6.0 < M < 7.0$, (d) $7.0 < M < 8.0$, (e) $8.0 < M <$
 905 10.0 , (f) $10.0 < M < 12.0$, (g) $12.0 < M < 20.0$, and (h) $20.0 < M < 68.0$.

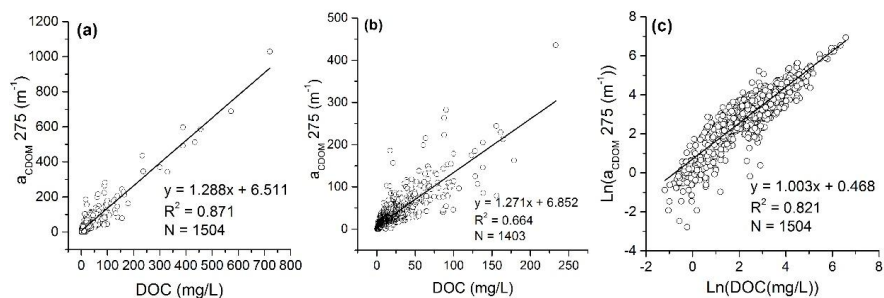
906
907



908
909
910
911
912
913
914
915
916
917
918
919
920
921
922
923
924
925



926 Fig.9. the relationships between $a_{CDOM,275}$ and DOC concentrations. (a) regression
927 model with pooled dataset; (b) regression model with DOC concentration less than
928 300 mg/L; (c) regression model with natural logarithmic transformed data.



929

930

931

932

933

934

935

936

937

938

939

940

941

942

943

944

945

946 **Tables**

947

948 Table 1. Water quality in different types of waters, DOC, dissolved organic carbon;

949 EC, electrical conductivity; TP, total phosphorus; TN, total nitrogen; TSM, total

950 suspended matter; Chl-a, chlorophyll-a concentration.

		DOC (mg/L)	EC μs/cm	pH	TP (mg/L)	TN (mg/L)	TSM (mg/L)	Chl-a (μg/L)
FW	Mean	10.2	434.0	8.2	0.5	1.6	67.8	78.5
	Range	1.9-90.2	72.7-1181.5	6.9-9.3	0.01-10.4	0.001-9.5	0-1615	1.4-338.5
SW	Mean	27.3	4109.4	8.6	0.4	1.4	115.7	9.0
	Range	2.3-300.6	1067-41000	7.1-11.4	0.01-6.3	0.6-11.0	1.4-2188	0-113.7
RW	Mean	8.3	10489.1	7.8-9.5	-	-	-	-
	Range	0.9-90.2	3.7-1000	8.6	-	-	-	-
UW	Mean	19.44	525.4	8.0	3.4	3.5	50.5	38.9
	Range	3.5-123.3	28.6-1525	6.4-9.2	0.03-32.4	0.04-41.9	1-688	1.0-521.1
WW	Mean	67.0	1387.6	8.1	0.7	4.3	181.5	7.3
	Range	7.3-720	139-15080	7.0-9.7	0.1-4.8	0.5-48	9.0-2174	1.0-159.4
IMW	Mean	6.7	242.8	8.3	0.19	1.1	17.4	1.1
	Range	0.3-76.5	1.5-4350	6.7-10	0.02-2.9	0.3-8.6	0.3-254.6	0.28-5.8

951

952 Note: FW, fresh water lake; SW, saline water lake, RW, river or stream water; UW, urban water;

953 WW, ice covered winter water from Northeast China; IMW, ice melt water from Northeast China.

954

955

956

957

958

959

960

961

962

963

964

965

966

967

968

969

970

971

972

973



974 Table 2. Descriptive statistics of dissolved organic carbon (DOC) and $a_{\text{CDOM}(440)}$ in
 975 various types of waters.

976

Type	Region	DOC				$a_{\text{CDOM}(440)}$			
		Min	Max	Mean	S.D	Min	Max	Mean	S.D
River	Liaohe	3.6	48.2	14.3	9.49	0.46	3.68	0.92	0.58
	Qinghai	1.2	8.5	4.4	1.96	0.13	2.11	0.54	0.63
	Inner M	16.9	90.2	40.4	24.84	0.32	7.46	1.03	2.11
	Songhua	0.9	21.1	8.1	4.96	0.32	18.93	3.2	4.19
Saline	Qinghai	1.7	130.9	67.9	56.7	0.13	0.86	0.36	0.23
	Hulunbir	8.4	300.6	68.5	69.2	0.82	26.21	4.41	4.45
	Xilinguo	3.74	45.4	14.2	8.8	0.36	4.7	1.34	0.88
	Songnen	3.6	32.6	16.4	7.4	0.46	33.80	2.4	3.78

977
 978
 979
 980
 981
 982
 983
 984
 985
 986
 987
 988
 989
 990
 991
 992
 993
 994
 995
 996
 997
 998
 999
 1000
 1001



1002 Table 3. Fitting equations for DOC against $a_{CDOM}(275)$ in different types of waters

1003 except ice covered lake underlying water and ice melting waters.

Water types	Region or Basin	Equations	R ²	N
Freshwater lakes	Northeast Lake Zone	$y = 3.13x - 3.438$	0.87	102
	North Lake Zone	$y = 2.16x - 1.279$	0.90	63
	East Lake Zone	$y = 1.98x + 7.813$	0.66	69
	Yungui Lake Zone	$y = 1.295x - 44.56$	0.71	54
Saline lakes	Songnen Plain	$y = 2.383x + 1.101$	0.92	159
	East Mongolia	$y = 1.791x + 8.560$	0.67	57
	West Mongolia	$y = 1.133x + 3.900$	0.81	46
	Tibetan Plateau	$y = 0.864x + 2.255$	0.84	83
Rivers or streams	Branch of the Nenjiang River	$y = 7.655x - 42.64$	0.81	33
	Songhua River stem	$y = 3.759x - 6.618$	0.71	29
	Branch of Songhua River	$y = 8.496x - 12.14$	0.98	33
	Liao River Autumn 2012	$y = 1.099x + 3.900$	0.80	38
	Liao River Autumn 2013	$y = 1.073x - 4.157$	0.88	28
	Liao River Spring 2013	$y = 2.262x - 10.32$	0.85	25
	Rivers from North China	$y = 3.154x - 1.207$	0.87	48
	Rivers from East China	$y = 3.037x - 2.585$	0.88	47
Rivers from Tibetan	$y = 2.345x + 2.375$	0.87	41	
Urban waters	Waters from Changchun	$y = 2.471x - 2.231$	0.54	48
	Waters from Harbin	$y = 1.413x - 4.521$	0.67	31
	Waters from Beijing	$y = 0.874x + 11.12$	0.63	27
	Waters from Tianjin	$y = 0.994x + 7.368$	0.57	23

1004

1005

1006